The Eurasia Proceedings of Science, Technology, Engineering & Mathematics (EPSTEM)
ISSN: 2602-3199

The Eurasia Proceedings of Science, Technology, Engineering & Mathematics (EPSTEM), 2020

Volume 11, Pages 9-13

IConTES 2020: International Conference on Technology, Engineering, and Science

Resistance Spot Welding of ZAMAK 12

Osman TORUN
Afyon Kocatepe University

Bedri BAKSAN
Eskişehir Osmangazi University

Ibrahim CELIKYUREK
Eskişehir Osmangazi University

Abstract: Zamak 12 offers high hardness and high tensile strength. This is the preferred alloy for permanent mold applications although it can also be cold-chamber die-cast with excellent results. It combines low temperature melting efficiency and thin wall capabilities with premium mechanical properties. ZA-12 can usually be poured directly into molds designed for aluminum and brass. In this work, the weldability of the ZA-12 alloy using the resistance spot welding technique was investigated. The alloy was melted in a melting furnace and casted in a sand mold. The resistance spot welding processes were carried out using the welding current of 3 kA and the welding times of 30, 40, 50 cycles under the electrode loads of 500 N. The microstructures of the interfaces of welded samples were examined with light optical microscopy (LOM). The tensile-shear tests were carried out at room temperature to determine weld strength. The welding time affected slightly the welding strength. The hardness of the welding zone and matrix was measured. The hardness of the weld interface and base material was similar for all welding conditions.

Keywords: Zamak 12, Hardness, Welding

Introduction

Various welding methods are used in manufacturing industries such as gas tungsten arc welding, submerged arc welding, shielded metal arc welding, flux core arc welding, and resistance spot welding. Among them, resistance spot welding is widely used in manufacturing processes due to its easy applicability and low equipment cost (Vural and Akkus, 2004). In the RSW method, overlapping plates are placed between two electrodes, and heat is obtained by passing a large electric current for a short time (Pouranvari and Marashi, 2011). Then, the electrical resistance at the metal interface causes local heating for the joint and finally melting. In the literature, there is a lot of study on resistance spot welding such as steel (Shirmohammadi et al., 2017), aluminum alloys (Florea et al., 2012), magnesium alloys (Niknejad et al., 2014), titanium alloys (Kahraman, 2007), iron/aluminum (Qiu et al., 2009) and (Bemani and Pouranvari, 2020). Zinc-Aluminum based alloys (ZAMAK) have become interesting in many industrial applications in recent years due to their advantages such as high wear resistance, high specific strength, easy and economical production (Fatile et al., 2017; Şevik, 2014; Shivakumar et al., 2017).

Zamak alloys, which have a high usage area in the building used widely in automotive sectors, in electronic devices. It is frequently preferred in household goods, ready-to-wear, toys, sports, business machines, hardware, agriculture, and mining (Polat 2009). The most common zinc-aluminum alloy (ZAMAK, ZA, ALZEN) are ZA-8, ZA-12, and ZA-27 alloys. These alloys contain higher amounts of aluminum than other ZAMAK alloys. Since the casting quality will increase with increasing Al concentration, better engineering properties can be obtained. A small amount of some alloying elements (Cu, Mg, Si, Ni) improve the mechanical and tribological properties of the cast ZA alloys (Ayday,2018).

- Selection and peer-review under responsibility of the Organizing Committee of the Conference

A high-quality joint of zinc-based die-cast alloys can be hardly achieved by conventional fusion welding. In this study, Zamak 12 alloy was welded using the resistance spot welding and examined microstructure and determined mechanical properties.

Method

Zinc alloy ZAMAK-12 was produced by an induction melting furnace at the nominal composition of 88%Zn, 11.0%Al, and 1.0%Cu (wt%). Firstly, Zn was melted, then Al was added, finally, Cu was dissolved in the melt. The melted liquid was stirred slowly using a steel rod. After obtaining a homogenous mixture the alloy was gravity casted into a graphite mold. Then, obtained rectangular form samples were hot-rolled until the thickness of samples has 1 mm. The dimensions of the samples for the resistance spot welding processes were prepared to be 40x10x1 mm3. The welding processes were performed for 30, 40, and 50 cycles under the compression time of 40 cycles, the welding current of 3 kA, and the electrode load of 500 N. A fixture was prepared to prevent the overlapping plates from slipping from the axis during the welding process (Figure 1).

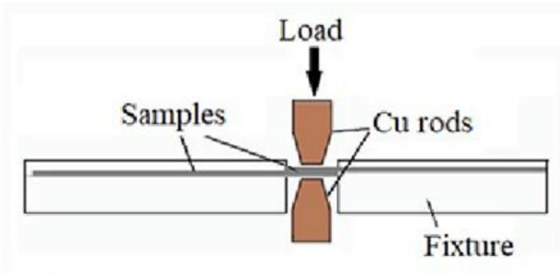

Figure 1. Resistance spot welding geometry.

The welding processes were carried out in a water-cooled and pneumatically controlled spot resistance welding machine. A schematic illustration of the resistance spot welding process was given in Fig 1. The microstructural and mechanical properties of the welded samples were investigated under experimental conditions. For this purpose, four samples were prepared for each test parameter. One of them was cut from the center of the melting zone (nugget) and molded for metallographic examinations, the others were used for mechanical characterization. The molded sample was grounded and polished with 1 µm diamond paste, then the samples were etched with nital %3. The welding interface of the samples was examined using light optical microscopy. The hardness measurements were carried out by applying a load of 300 gr. with Shimadzu HMV type device.
Three welded samples were subjected to a tensile test in a Shimadzu AGIS tensile-compression testing device for each welding parameter. The tests were carried out at room temperature with a loading speed of 5 mm/min. The schematic illustration of the test geometry was given in Fig. 2. The welding interface strength was determined by taking the average of three samples.

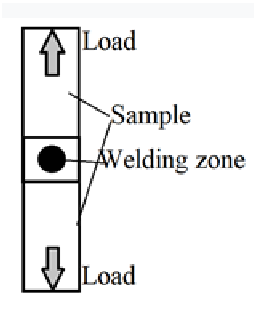

Figure 2. The tensile test geometry of the welding zone.

Results and Discussion

Optical microscope photos of the welded samples for 30, 40, and 50 cycles at a welding current of 3kA under electrode force of 500 N are given in Fig.3. It is clearly seen that a nugget region is formed at the interface of the welded samples for all welding times from photographs. New grains have formed in the nugget zone occurred at the interface of welded samples. The grain shape in the nugget zone is equ-axial. Normally, while the matrix material has axially elongated grains, after welding, equ-axial grains were formed at the welding interface. The nugget zone was expanded with an increase in welding time. The increase in welding time caused an increase in the heat input in the interface of welded samples. More melting occurred at the interface of the welded samples. As a result of this situation the nugget zone expanded.

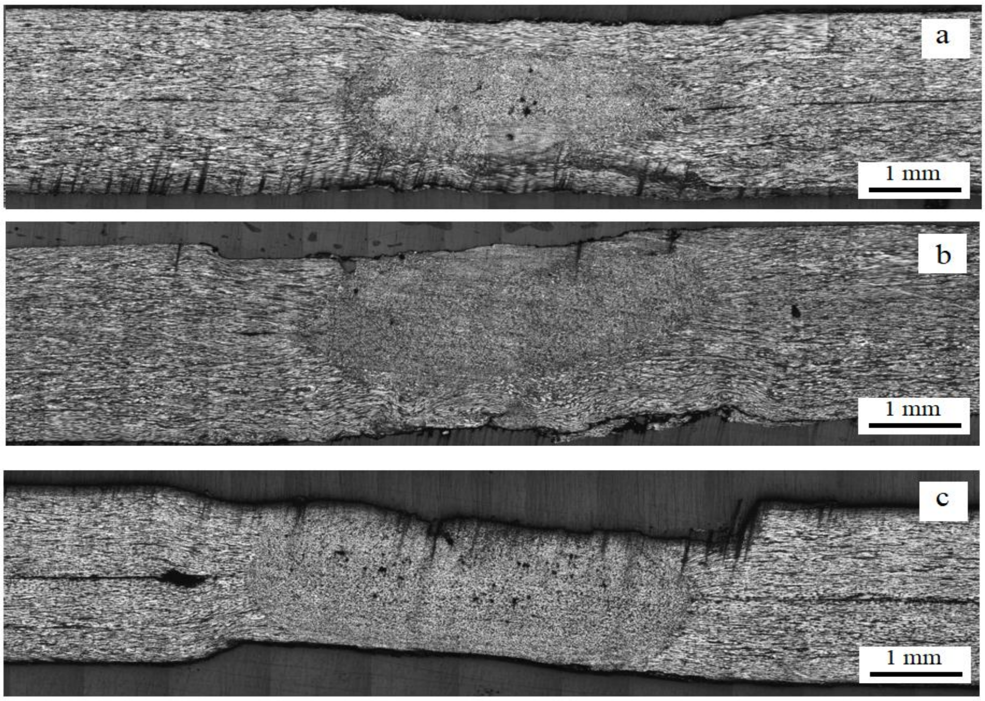

Figure 3. Optical micrographs of welded samples. a) 30 cycle b) 40 cycle c) 50 cycle

As shown schematically in Fig. 4 the microhardness values of the samples were measured from the center of the nugget zone to both sides of the matrix. The hardness values are given in Figure 5. As can be seen from the figure, in the hardness values of the nugget and the heat-affected zone no significant change was observed.

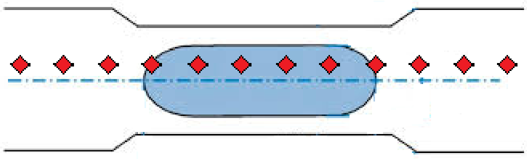

Figure 4. Schematic illustration of hardness measurement

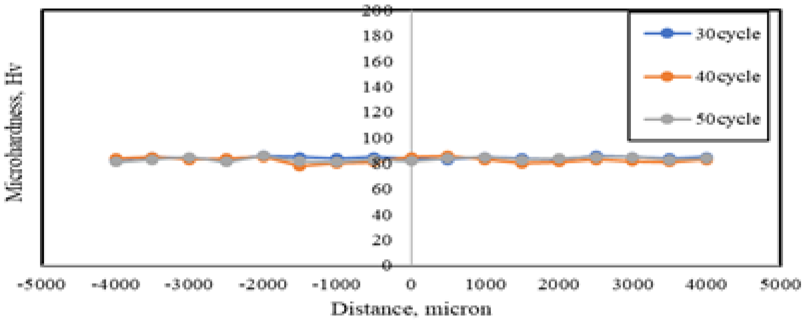

Figure 5. The hardness variation of the welding zone and matrix.

Tensile-shear tests were performed out an electromechanical universal testing machine with a speed of 5 mm/min at room temperature. The strength values obtained in the tests were given in Figure 6. The test results show that shear force values increase with increases in the welding time in the welded samples. The heat input increased with the increase in welding time and the nugget zone expanded. Thus, more melting occurred on the surfaces contacting the interface of the welded samples. As a result, the sheer force slightly increased with increasing the welding time.

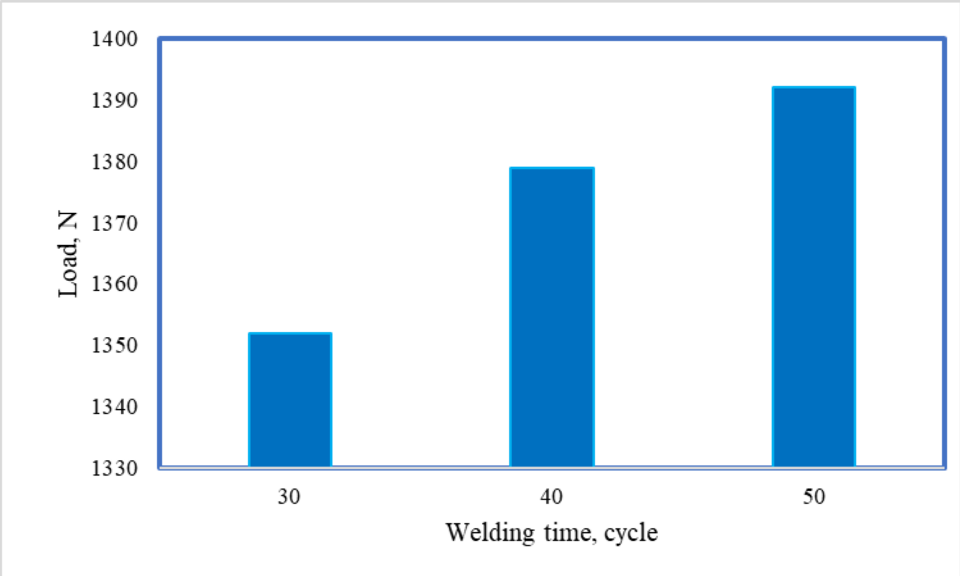

Figure 6. The strength values of the welded samples

Conclusion

In this study, the resistance spot welding of ZAMAK 12 was carried out using the welding current of 3 kA and the welding times of 30, 40, 50 cycles under the electrode loads of 500 N. A crack-free and oxide-free weld interface in microstructural studies observed. With the increase in welding time, the heat input increased and as a result of this situation, the nugget zone expanded. The microhardness values of the weld zone and the matrix structure were measured close to each other and there was no significant change in the hardness values. The shear forces of the welded specimens increased depending on the welding time and the highest shear force was found as 1392 N for 30 cycles.

References

Ayday A., (2018). Çinko-Alüminyum esaslı ZA-12 alaşımının mikroyapı ve darbe dayanımına bor elementinin etkisi, *BAUN Fen Bil. Enst. Dergisi*, *20*(1), 243-249.

Bemani M., Pouranvari M. (2020) Microstructure and mechanical properties of dissimilar nickel-based superalloys resistance spot welds, *Mater. Sci. Eng. A. 773*, 138825.

Fatile B.O., Adewuyi B.O., and Owoyemi H.T.(2017). Synthesis and characterization of ZA-27 alloy matrix composites reinforced with zinc oxide nanoparticles, *Engineering Science and Technology*. *11*, 47–1154.

Florea R.S., Solanki K.N., Bammann D.J., Baird J.C., Jordon J.B., Castanier M.P. (2012). Resistance spot welding of 6061-T6 aluminum: Failure loads and deformation. *Materials and Design 34*, 624–630.

Kahraman N. (2007). The influence of welding parameters on the joint strength of resistance spot-welded titanium sheets. *Mater Des, 28*:420–7.

Niknejad S., Liu L., Lee M., Esmaeili S., Zhou N. Y. (2014). Resistance spot welding of AZ series magnesium alloys: Effects of aluminum content on microstructure and mechanical properties *Mater. Sci. Eng. A 618*, 323–334.

Polat B.D.(2009). Zamak alaşımı nedir? Zamaktan nasıl para kazanılır? *Metalürji Dergisi*, sayı 159.

Pouranvari M, Marashi SPH (2011). Failure mode transition in AHSS resistance spot welds. Part I. Controlling factors. *Mater Sci Eng A; 528*:8337–43.

Qiu R, Iwamoto C, Satonaka S. (2009). Interfacial microstructure and strength of steel/aluminum alloy joints welded by resistance spot welding with cover plate. *J Mater Process Technol. 209*:4186–93.

Shirmohammadi D., Movahedi M., Majid P. (2017). Resistance spot welding of martensitic stainless steel: Effect of initial base metal microstructure on weld microstructure and mechanical performance, *Mater. Sci. Eng. A 703*,154–161.

Shivakumar, N., Vasu, V., and Narasaiah N. (2017). Processing and dry sliding wear behavior of Al2O3 nanoparticles reinforced ZA-27 composites, *Materials Today*: Proceedings, 4, 4006–4012.

Şevik H. (2014). The effect of silver on wear behavior of zinc–aluminum-based ZA-12 alloy produced by gravity casting, *Materials Characterization, 89,* 81–87.

Vural M, Akkus A. (2004). On the resistance spot weldability of galvanized interstitial free steel sheets with austenitic stainless steel sheets. *J Mater Process Technol, 153*–154:1–6.

Author Information

Osman TORUN
Afyon Kocatepe University
Afyon Kocatepe University, Technology Faculty,
Department of Mechatronic Engineering
otorun@aku.edu.tr

Bedri BAKSAN
Eskişehir Osmangazi University
Eskişehir Osmangazi University, Department of Metallurgy and Materials Engineering

İbrahim ÇELİKYÜREK
Eskişehir Osmangazi University
Eskişehir Osmangazi University, Department of Metallurgy and Materials Engineering